COMBINING TIME TRANSFER MEASUREMENTS USING A KALMAN FILTER

J. A. Davis, P. W. Stacey, P. M. Harris, and M. G. Cox
National Physical Laboratory, Queens Road, Teddington
Middlesex TW11 0LW, UK

Abstract

Time transfer measurements made between UTC (k) timing laboratories are routinely performed using a variety of satellite-based methods. The National Physical Laboratory has undertaken a study of combining time transfer measurements from separate links between two laboratories, where each link measures the same clock difference. The aim is to produce a time series of (composite) time-transfer measurements that has appreciably less measurement noise than any of the component measurements. A Kalman filter is used to combine the measurements. The method is developed to treat some of the known characteristics of satellite time transfer measurements. These include time series having different measurement intervals, and slowly changing delays occurring within the time transfer hardware. The treatment of missing data and the addition and removal of individual links are also examined.

1. INTRODUCTION

Time scales at timing laboratories generating Coordinated Universal Time (UTC (k)) are routinely compared using a variety of satellite-based methods including TWSTFT **[1]**, geodetic GPS **[2]**, P3 and C/A code GPS common view **[3],** and GLONASS common view **[4]**. Many of the larger UTC (k) laboratories use all the above methods operationally as well as having considerable redundant hardware. Time transfer links used in the formation of UTC by the Bureau International des Poids et Mesures (BIPM) are processed using measurements obtained from one particular time transfer technique, employing only a single set of hardware. Improvement would be expected by processing all the available time transfer measurements.

This paper describes a study undertaken at the National Physical Laboratory (NPL) of combining time transfer measurements made between two laboratories using several different methods and more than one set of hardware for each method. The aim is to produce, over the short and long term, composite time transfer measurements having time and frequency uncertainties that are smaller than those for any individual set of measurements. A further objective is to provide an approach that is sufficiently flexible to handle a variety of practical circumstances.

A description of an algorithm based on a Kalman filter to combine the measurements is given in Section 2. Some of the extensive tests of the algorithm using simulated data are discussed in Section 3. The process of adding and removing time transfer links is considered in Section 4. In Section 5 the filter is applied to time transfer links that provide measurements with different minimum spacing. The treatment of missing data is also considered. Future possible modifications to the filter are discussed in Section 6. The conclusions to this study are presented in Section 7.

2. TIME TRANSFER ALGORITHM BASED ON A KALMAN FILTER 3.

3.1 INTRODUCTION

A Kalman filter is an iterative algorithm that produces estimates of physical parameters (comprising a so-called state vector) at the current epoch by combining measurements made at that epoch with estimates of those parameters determined at the previous epoch. The application of a Time Transfer Kalman Filter (TTKF) algorithm to combine a number of time transfer measurements should in principle be relatively straightforward, as, in contrast to a clock algorithm **[6],** the physical parameters can be measured directly.

There are, however, several aspects of time transfer measurements that make its application more complicated. These include (a) slowly changing delay biases that may occur on each of the individual time transfer links, (b) a wide variety of noise processes present in both the time transfer measurements and the clocks being compared, (c) measurement data sets that have a wide variety of minimum spacing and are often incomplete, and (d) significant correlations that may exist between the measurements obtained from individual links. In addition, the filter must be designed so that a link can be added and removed, in the latter case without appreciably degrading the filter's performance.

NPL's approach to this study was to start with an idealized model of time transfer measurements, the resulting Kalman filter being evaluated using simulated data. New elements or properties were then added in turn to the TTKF algorithm to treat more physically realistic situations.

Let $\mathbf{x}(t_n)$ be a vector of values of the physical parameters being estimated by the Kalman filter at the current epoch t_n. The evolution of these physical parameters is modelled by the state equation

$$\mathbf{x}(t_n) = \Phi(\tau_0)\mathbf{x}(t_{n-1}) + \varepsilon(t_n), \tag{1}$$

where $\Phi(\tau_0)$ is the state propagation matrix and $\boldsymbol{\varepsilon}(t_n)$ the system error in the state equation, τ_0 being the interval between successive measurement epochs. The relationship between $\mathbf{y}(t_n)$, the measurements made at t_n, and $\mathbf{x}(t_n)$ is given by the observation equation

$$\mathbf{y}(t_n) = H(t_n)\mathbf{x}(t_n) + \mathbf{e}(t_n), \tag{2}$$

where $H(t_n)$ is the design matrix and $\mathbf{e}(t_n)$ the observation error at epoch t_n. The system errors and observation errors at t_n may respectively be described in terms of the process covariance matrix $Q(t_n)$ and measurement covariance matrix $R(t_n)$, where

$$Q(t_n) = E(\varepsilon\varepsilon^{\mathrm{T}}), \quad \varepsilon = \varepsilon(t_n), \tag{3}$$

$$R(t_n) = E(\mathbf{e}\mathbf{e}^{\mathrm{T}}), \quad \mathbf{e} = \mathbf{e}(t_n), \tag{4}$$

and E is the expectation operator.

The standard iterative Kalman filter equations **[5]** are then given by

$$\hat{\mathbf{x}}(t_n^-) = \Phi(\tau_0)\hat{\mathbf{x}}(t_{n-1}^+), \tag{5}$$

$$P(t_n^-) = \Phi(\tau_0) P(t_{n-1}^+) \Phi^{\mathrm{T}}(\tau_0) + Q(t_n), \tag{6}$$

$$K(t_n) = P(t_n^-) H^{\mathrm{T}}(t_n) \left[H(t_n) P(t_n^-) H^{\mathrm{T}}(t_n) + R(t_n) \right]^{-1}, \tag{7}$$

$$\hat{\mathbf{x}}(t_n^+) = \hat{\mathbf{x}}(t_n^-) + K(t_n) \left[\mathbf{y}(t_n) - H(t_n) \hat{\mathbf{x}}(t_n^-) \right], \tag{8}$$

$$P(t_n^+) = \left[I - K(t_n) H(t_n) \right] P(t_n^-), \tag{9}$$

where $\hat{\mathbf{x}}(t_n^-)$ and $\hat{\mathbf{x}}(t_n^+)$ represent the state vector at the current epoch before and after the incorporation of the current measurements, $P(t_n^-)$ and $P(t_n^+)$ the associated covariance matrices, and $K(t_n)$ is the Kalman gain.

3.2 Choice of State Vector

The key to the design of a good Kalman filter is the choice of the physical parameters that constitute the state vector $\hat{\mathbf{x}}(t_n)$. A natural choice in this application is $\hat{\mathbf{x}}(t_n) = (\hat{x}_{a0}, \hat{x}_{a1}, \hat{x}_{a2})^{\mathrm{T}}$, where $\hat{x}_{a0}$ is the time offset, $\hat{x}_{a1}$ the frequency offset, and $\hat{x}_{a2}$ the linear frequency drift offset between the two UTC (k) timescales being assessed. A consequence of this choice is that the two scales have the characteristics of free-running clocks. It is therefore important to "back correct" the UTC (k) data to remove any steers so that it is obtained directly from a free-running clock or timescale.

Figure 1 shows plots of UTC (NPL) − UTC (USNO) made using TWSTFT (TW), geodetic GPS (CP), and GPS common-view (CV) time transfer links. Figure 2 shows the differences between the measurements for each pair of links. Taking differences eliminates the clock noise. There are clearly biases associated with the links; these are observed as offsets between the measurements obtained from two independent links. These biases are initially due to calibration errors, but their magnitude may increase due to instabilities associated with slow random delay occurring within the time transfer instrumentation. In the TTKF algorithm presented here, these biases are considered to be physical parameters and described by *m* additional elements of the state vector, one for each link, where *m* is the number of links. The complete state vector is therefore given by

$$\hat{\mathbf{x}}(t_n) = (\hat{x}_{a0}, \hat{x}_{a1}, \hat{x}_{a2}, \hat{x}_{b1}, .., \hat{x}_{bm})^{\mathrm{T}}, \tag{10}$$

i.e., by augmenting the original vector by bias terms $\hat{x}_{b1}, .., \hat{x}_{bm}$. Introducing these extra elements complicates the operation of the Kalman filter. The situation is reminiscent of a clock algorithm where the physical parameters constituting the state vector are not measured directly. In this case, element $\hat{x}_{a0}$ and the elements of $\hat{x}_b$ may become confounded.

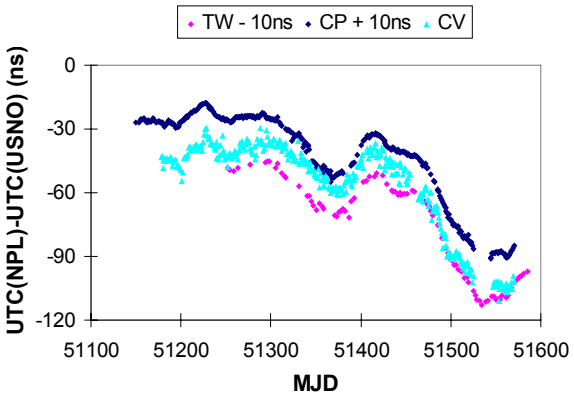

Figure 1. Plots of UTC (NPL) – UTC (USNO) measured using three different time transfer links.

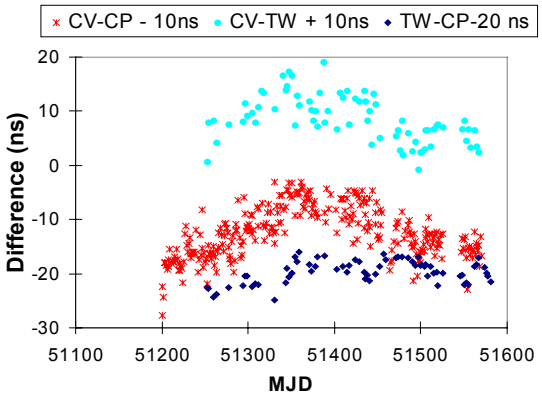

Figure 2. Plots of the difference between measurements obtained from pairs of UTC (NPL) – UTC (USNO) time transfer links.

3.3 State Propagation Matrix

The first Kalman filter equation (5) determines the state vector at the current epoch using only measurements already incorporated into the filter from previous epochs. Key to this process is the use of the $(m+3)\times(m+3)$ state propagation matrix Φ. The physical parameters at the current epoch are estimated by extrapolating estimates of these parameters made at the previous epoch on the basis of the underlying quadratic model that follows from the choice of parameters made in Section 2.2. Φ describes the deterministic relationship between the physical parameters at consecutive epochs. The form of Φ used in the TTKF algorithm is given in equation (11).

$$\Phi = \begin{pmatrix} 1 & \tau_0 & \frac{\tau_0^2}{2} & 0 & \Lambda & \Lambda & 0 \\ 0 & 1 & \tau_0 & \mathrm{M} & & & \mathrm{M} \\ 0 & 0 & 1 & 0 & \Lambda & \Lambda & 0 \\ 0 & \Lambda & 0 & 1 & 0 & \Lambda & 0 \\ \mathrm{M} & & \mathrm{M} & 0 & 1 & & 0 \\ \mathrm{M} & & \mathrm{M} & \mathrm{M} & & \mathrm{O} & \mathrm{M} \\ 0 & \Lambda & 0 & 0 & 0 & \Lambda & 1 \end{pmatrix}. \qquad (11)$$

The leading 3×3 sub-matrix of Φ describes the changes in the time-offset, frequency-offset, and linear frequency-drift-offset state vector elements due to the deterministic properties of the clocks being compared. This state propagation matrix has been used extensively in clock algorithms **[6]**. The bottom right $m\times m$ sub-matrix is the identity matrix of order m. It is assumed that there are no deterministic processes that change the bias elements of the state vector. The consequent assumption is that changes to the time-transfer instrumentation delays are due only to random processes.

3.4 PROCESS COVARIANCE MATRIX FOR ERRORS IN THE STATE EQUATION

The second Kalman filter equation (6) determines the covariance matrix $P(t_n^-)$ of order $m+3$ for the prediction $\hat{\mathbf{x}}(t_n^-)$ at the current epoch, before the measurements are incorporated in the filter. The process covariance matrix Q (equation (12)), also of order $m+3$, describes the noise processes that result in changes to the physical processes between successive epochs that are estimated by the state vectors.

$$Q=\begin{pmatrix} \sigma^2_{\mathrm{WFM}}\tau_o+\sigma^2_{\mathrm{RWFM}}\tau_0^3/3, & \sigma^2_{\mathrm{RWFM}}\tau_0^2/2, & 0 & 0 & \Lambda & 0 \\ \sigma^2_{\mathrm{RWFM}}\tau_0^2/2, & \sigma^2_{\mathrm{RWFM}}\tau_o, & 0 & \mathrm{M} & & \mathrm{M} \\ 0 & 0 & 0 & 0 & \Lambda & 0 \\ 0 & \Lambda & 0 & \sigma^2_{b11} & \Lambda & \sigma^2_{b1m} \\ \mathrm{M} & & \mathrm{M} & \mathrm{M} & & \mathrm{M} \\ 0 & \Lambda & 0 & \sigma^2_{bm1} & \Lambda & \sigma^2_{bmm} \end{pmatrix}. \qquad (12)$$

The leading 3 × 3 sub-matrix of Q is the well-known process covariance matrix used in clock algorithms, where σ^2_{WFM} and σ^2_{RWFM} are the variances of the White Frequency Modulation (WFM) and Random Walk Frequency Modulation (RWFM) noise parameters **[7]**. The bottom right $m \times m$ sub-matrix is the covariance matrix B of order m of the bias state vectors. The long-term instability of these biases is modelled as a random-walk process that resembles WFM. In reality, modelling these instabilities as a flicker-phase process may be more appropriate, an option that will be considered in future work. The magnitude of the delay instabilities will be very much smaller than the variance of the WFM clock noise. The remaining elements of Q are zero, since it is assumed that the clock noise and delay instabilities of the time transfer links producing the biases are uncorrelated.

Design Matrix

The $(m+1) \times (m+3)$ design matrix $H(t_n)$ describes the relationship between the measurements $\mathbf{y}(t_n)$ and the state vector $\hat{\mathbf{x}}(t_n)$ at t_n. Expression (13) is the choice of $H(t_n)$ used in the TTKF algorithm. In the first implementation of the filter in the NPL study, $H(t_n)$ had only the first m rows in expression (13), corresponding to a measurement made with m particular time transfer links. As stated (Section 2.2), when using this design matrix, the elements $\hat{x}_{a0}$ and $\hat{x}_{b1}, \mathrm{K}, \hat{x}_{bm}$ of the state vector become confounded. This, coupled with the time transfer bias instabilities being modelled as nonstationary WFM noise processes, results in the time-offset element P_{11} of the covariance matrix P increasing indefinitely. Physically this corresponds to the uncertainty of the resulting time transfer estimate increasing with time due to the cumulative effects of the instrumentation delay instabilities of each of the time transfer links. Although physically realistic, operating a Kalman filter in this configuration may not be desirable. Because the magnitude of the instabilities in the bias state vectors is very small the "covariance growth" is unlikely by itself to be a problem when operating the filter.

$$H = \begin{pmatrix} 1 & 0 & 0 & 1 & 0 & \Lambda & 0 \\ 1 & 0 & 0 & 0 & 1 & \Lambda & 0 \\ \mathrm{M} & \mathrm{M} & \mathrm{M} & \mathrm{M} & \mathrm{M} & \mathrm{O} & \mathrm{M} \\ 1 & 0 & 0 & 0 & 0 & \Lambda & 1 \\ 0 & 0 & 0 & w_1 & w_2 & \Lambda & w_m \end{pmatrix} \tag{13}$$

In later versions of the filter, $H(t_n)$ was augmented by a "pseudo-measurement," viz., as the last ($(m + 1)^{st}$) row in expression (13). All the corresponding measurements $y_{m+1}(t_n)$ are set to a constant K_w that is initially taken as zero. K_w is changed only when time transfer links are added or removed from the algorithm. The weights $\mathbf{w}^{\mathrm{T}} = (w_1,..,w_m)^{\mathrm{T}}$ are determined by

$$\mathbf{w} = \frac{B^{-1}\mathbf{1}}{\mathbf{1}^T B^{-1}\mathbf{1}}, \tag{14}$$

where B is the bottom right $m \times m$ sub-matrix of the process covariance matrix Q. This weighting scheme minimizes the effect of the long-term instabilities present in the time transfer measurements.

The pseudo-measurement acts as a constraint that improves the performance of the TTKF algorithm in several ways:

a) The state vectors are explicitly determined from the available "measurements."
b) "Covariance growth" is prevented.
c) The stability of the filter is improved.
d) The weights minimize the effects of delay instabilities in the time transfer instrumentation.
e) It is easier to add and remove time transfer links.

A disadvantage is that the prevention of "covariance growth" implies that the covariance matrix P is no longer a valid measure of the uncertainty in the state vector estimates of the physical parameters.

3.5 Measurement Covariance Matrix for Errors in the Observations

The measurement covariance matrix R characterizes the noise processes occurring within the time transfer measurements. The long-term instabilities due to delay changes in the time transfer instrumentation have already been modelled as part of the process covariance matrix Q. It is assumed that the remaining noise is principally WPM. Correlation between the noise of individual time transfer links may be described by adding nonzero off-diagonal elements. Element $R_{m+1,m+1}$ represents the variance of the "noise" in the pseudo-measurement and is initially set to a small finite value. Expression (15) gives the resulting covariance matrix used in the TTKF algorithm.

$$R = \begin{pmatrix} \sigma_{R11}^2 & \Lambda & \sigma_{R1m}^2 & 0 \\ \mathrm{M} & & \mathrm{M} & \mathrm{M} \\ \sigma_{Rm1}^2 & \Lambda & \sigma_{Rmm}^2 & 0 \\ 0 & \Lambda & 0 & \sigma_{Rc}^2 \end{pmatrix} \tag{15}$$

The remaining Kalman filter equations perform the following functions: Equation (7) provides the Kalman gain matrix *K*. This matrix specifies the weighting of each measurement made in the current epoch that is used in determining the state vector elements. Where the Kalman gain is low, measurements made at previous epochs have a greater influence in determining the current values of the state vector. Equation (8) is used to incorporate the measurements made at the current epoch into the state vector estimates. Equation (9) recomputes the covariance matrix *P* and, hence, the uncertainty in the state vector estimates following the incorporation of measurements at the current epoch.

4. PERFORMANCE OF THE ALGORITHM ON SIMULATED DATA

4.1 PARAMETERS USED IN THE STUDY

The results of a study of the performance of the TTKF algorithm are given here using simulated timetransfer and clock data. The underlying clock noise is assumed to be WFM with variance $\sigma^2_{\mathrm{WFM}} = 1.0$. The variance of the measurement noise for three of the time transfer links R_{11}, R_{22} and R_{33} (here called type A links) is taken as 2.0 and that for the three remaining links R_{44}, R_{55}, and R_{66} (type B links) as 0.5. The bias covariance matrix elements B_{11}, B_{22}, and B_{33} are set to 0.005 and the elements B_{44}, B_{55}, and B_{66} to 0.02. In this particular simulation, there is no correlation between individual time transfer links, although correlation effects have been examined in other simulations. This simulation deliberately considers links with (a) good short-term stability (measurement noise) and poor long-term stability (instrumentation delay instabilities) combined with (b) links having poor short-term stability and good long-term stability. The ability of an algorithm to combine links with such very different characteristics is a good test of its performance.

4.2 EVALUATION OF THE PERFORMANCE

Several possible statistics are available with which to evaluate the performance of the algorithm. Because this study uses simulated data, it is possible to evaluate $\hat{e}_1 = \hat{x}_{a0} - x$ at each epoch of the simulation where $\hat{x}_{a0}$ is the estimated time-offset state vector component and x the corresponding true (simulated) value. TDEV($\hat{e}_1$) was chosen as the main statistic for the following reasons:

a) It is widely used in the time and frequency community for characterizing time transfer links.
b) It is a statistic that can be used to evaluate the performance of the Kalman filter over the short and long term by using a variety of averaging times.

Other statistics may be considered in future work and include the magnitude of the time error $\hat{e}_1$.

4.3 SETTING THE INITIAL PARAMETERS

Initial estimates $\hat{\mathbf{x}}(t_1)$ and $P(t_1)$ of the state vector and covariance matrix are needed to start the TTKF algorithm. When the pseudo-measurements are included, it is possible to determine the initial values explicitly from the first few measurement epochs. Initial values of the time-offset state vector element and time-transfer bias state vector elements can be obtained from the measurements at the first epoch. Two and three epochs of measurements, respectively, are required to determine initial values of the frequency-offset and linear-frequency-offset state vector elements. The magnitudes of the elements of the

covariance matrix usually decrease as new measurements are included, finally reaching steady values. It proves to be satisfactory to set the elements of these matrices to relatively large values.

4.4 INITIAL RESULTS

Examples of the underlying clock noise and time-transfer link noise containing measurement noise and bias delay instabilities are shown in Figures 3 and 4 for a typical simulation. Plots of $\mathrm{Log}_{10}\mathrm{TDEV}(\hat{e}_1)$ against $\mathrm{Log}_{10}(\tau)$ for averaging times between 1 and 2,000 time units are shown in Figure 5 according to the data summarized in Table 1.

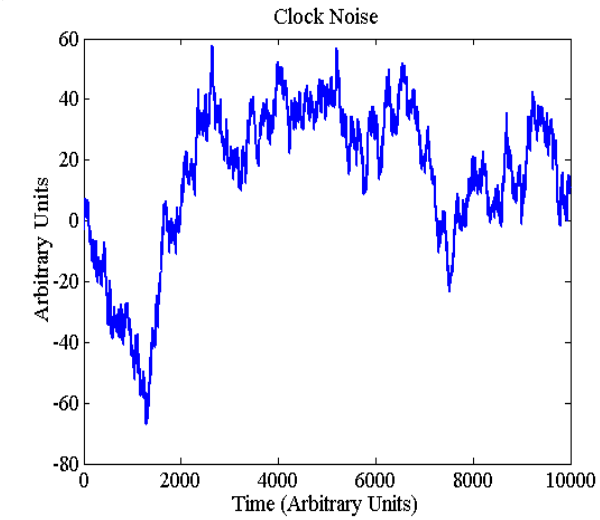

Figure 3. Example of simulated clock noise.

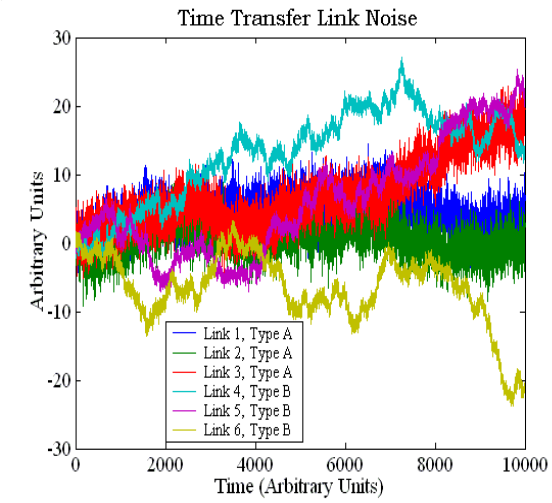

Figure 4. Example of simulated noise and instabilities originating from the time transfer instrumentation of six time transfer links.

The key results are summarized as follows:

1) Applying the Kalman filter to a single time transfer link with no pseudo-measurements does not always result in a smaller TDEV compared with that obtained by working directly with the raw time series. This suggests that the Kalman filter is not optimally configured.
2) Applying the filter to a group of three time transfer links with no pseudo-measurements results in smaller TDEV values *at all averaging times* compared with the value obtained by applying the filter to a single link.
3) Using the filter on a group of six time transfer links with no pseudo-measurements and where the links have very different characteristics results in a TDEV that *at almost all averaging times* is smaller than the best value obtained from applying the filter to three links.
4) Using a filter that includes pseudo-measurements improves the results further, particularly at intermediate averaging times.

Table 1. Nature of the data shown in Figure 5.

Data set	No. of time-transfer links	Filter applied?	Type of link	Pseudo-measurements?
A	1	No	A	—
B	1	No	B	—
C	1	Yes	A	No
D	1	Yes	B	No
E	3	Yes	A	No
F	3	Yes	B	No
G	6	Yes	A and B	No
H	6	Yes	A and B	Yes

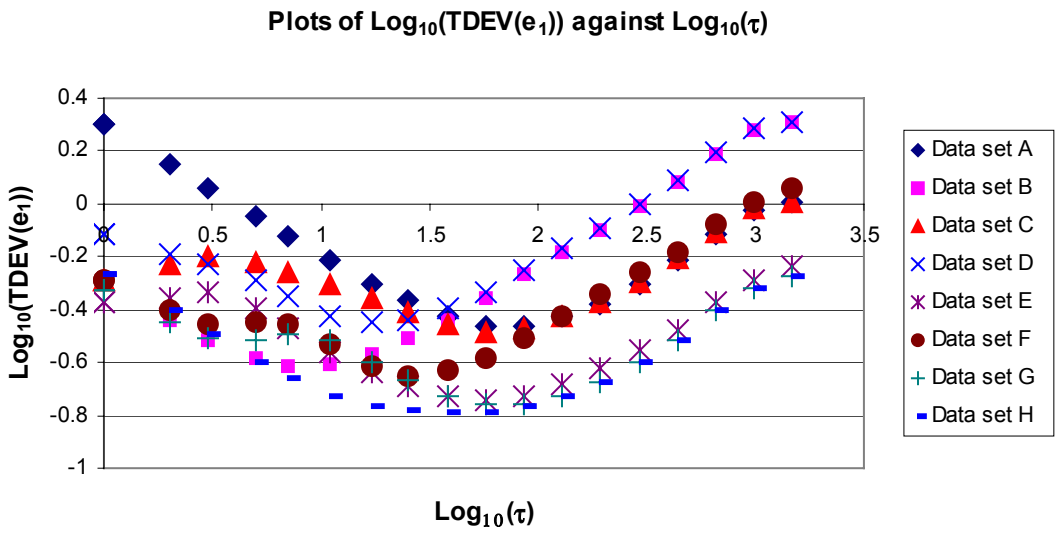

Figure 5. $\mathrm{Log}_{10}\mathrm{TDEV}(\hat{e}_1)$ plotted against $\mathrm{Log}_{10}(\tau)$.

The key conclusions drawn are:

1) With no pseudo-measurements the TTKF algorithm may perform sub-optimally.
2) With pseudo-measurements the TTKF algorithm produces a composite time transfer that is more stable *at almost all averaging times* than would be obtained by applying it to any subset of the component time-transfer links.

4.5 Limitations of the Above Results

Care must be exercised when interpreting the application of the above analysis to real time-transfer data for the following reasons:

1) In the study, the simulated clock and time transfer measurements contained noise that was either a pure integer noise type or a linear combination of such types. In practice, fractional noise types **[8]** and completely different noise structures, e.g., temperature-dependent effects, may occur.

2) The analysis assumes an exact knowledge of the noise parameters used in the process covariance matrix Q and the measurement covariance matrix R. In practice, these parameters must be estimated from the available measurements. Their estimation is discussed in Section 7 and has been studied previously **[9]**.

5. ADDITION AND REMOVAL OF TIME TRANSFER LINKS

For effective operation of the TTKF algorithm, it is required to add and remove time transfer links without introducing unnecessary steps in the output of the filter. The removal of a time transfer link is the simpler of the two processes.

5.1 LINK REMOVAL

To remove the k^{th} time-transfer link adjustments are made to the measurement vector **y** and the design matrix H. All the elements in the k^{th} row of H are set to zero as is the k^{th} element of **y.** An immediate consequence is that the bias state vector element $\hat{x}_{bk}$ will not be updated further. To preserve the performance of the filter over longer averaging times, the pseudo-measurement y_{m+1} and the associated $(m + 1)^{st}$ row of the design matrix are modified. A new set of bias weights $\mathbf{w}_R$ is determined from

$$\mathbf{w}_R = \frac{B_R^{-1}\mathbf{1}}{\mathbf{1}^T B_R^{-1}\mathbf{1}}, \tag{16}$$

where B_R is a covariance matrix of order $m - 1$ formed by removing the k^{th} row and column from the covariance matrix B. The weights $w^{\mathrm{T}} = (w_{R1},..,w_{R(k-1)},0,w_{Rk},..,w_{R(m-1)})^{\mathrm{T}}$ are then entered into the last row of the design matrix H. The pseudo-measurement is recalculated as

$$y_{m+1} = \sum_{i=1}^{m} w_i \hat{x}_{Bi} \tag{17}$$

5.2 LINK ADDITION

To add a link, an initial estimate of the state vector element $B_{(m+1)}$ and the elements $P_{B(m+1)}$ of the covariance matrix P is made. The bias weights and pseudo-measurement are updated in a similar way as when removing a link.

Examples of the addition and removal of time transfer links using simulated data are shown in Figures 6, 7, and 8. Figures 6 and 7 show the complete measurements and time transfer noise (both measurements and link instabilities), respectively. Figure 8 shows the time-offset error. The plots demonstrate that time-transfer links may be added and removed without introducing spurious steps to the value of the time-offset state vector element $\hat{x}_{a0}$.

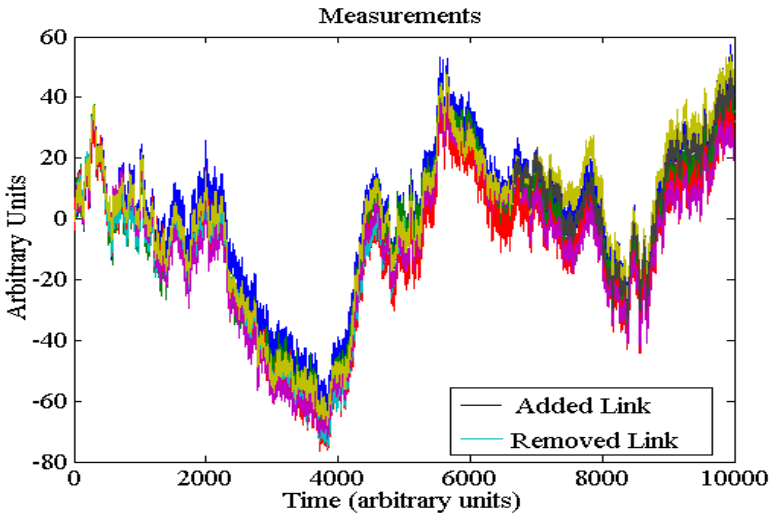

Figure 6. The simulated measurements. A time transfer link was removed at t = 5000 and added at t = 6500.

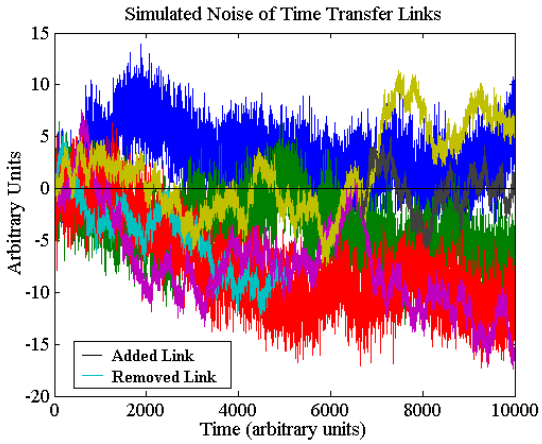

Figure 7. The simulated time transfer noise and link instabilities.

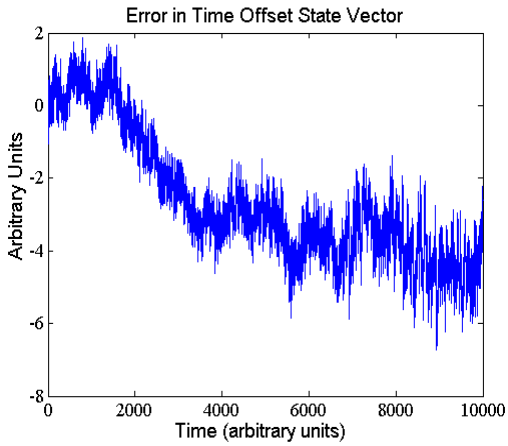

Figure 8. The error e_{a0} in the time-offset element of the state vector.

6. TIME TRANSFER LINKS WITH DIFFERENT MINIMUM SPACING

6.1 INTRODUCTION

Time-transfer links have a wide variety of minimum measurement interval. Geodetic GPS, common-view GPS, Ku-band TWSTFT, and X-band TWSTFT have minimum interval of 10 minutes, 16 minutes, 2–3 days (to be changed to 1 day), and 1 hour, respectively. Many links will also provide incomplete measurement time series. A TTKF algorithm must be able to combine such links.

6.2 EPOCHS WITH NO AVAILABLE MEASUREMENTS

The presence of j successive epochs (j arbitrary) with no available measurements can be handled by the TTKF algorithm. The state propagation matrix Φ and the process covariance matrix Q may be modified by replacing τ_0 by $(j+1)\tau_0$. Doing so effectively extrapolates the previous state vector over $j + 1$ epochs and updates the covariance matrix P accordingly.

6.3 PROCESSING DATA FROM EPOCHS WHERE THE MEASUREMENTS ARE INCOMPLETE

Adapting the TTKF algorithm to cope with incomplete measurements at any epoch is relatively straightforward. The measurement vector **y** and design matrix H are adjusted as follows: For each missing measurement y_i the value of y_i is set to zero, as are all elements in the i^{th} row of H. The pseudo-measurements and the corresponding row in H are left unaltered.

6.4 STUDIES USING SIMULATED DATA

A study of combining six time transfer links using simulated measurements was undertaken. The clock noise used was WFM with variance σ^2_{WFM} = 1.0. Time transfer links 1, 2, and 3 have spacing τ_0 (here called type C) and links 4, 5, and 6 have spacing $10\tau_0$ (type D). Measurements 4, 5, and 6 are assumed to be made simultaneously. The time transfer link noise and instabilities are not correlated. The measurement covariance matrix elements R_{11}, R_{22}, and R_{33} have the value 2.0 and elements R_{44}, R_{55}, and R_{66} the value 0.5. The link bias covariance matrix elements B_{11}, B_{22}, and B_{33} have the value 0.02 and elements B_{44}, B_{55}, and B_{66} the value 0.005. This example is deliberately constructed to have frequent, but noisy. measurements combined with less frequent, but much less noisy, measurements. It mimics the situation that arises in practice when combining TWSTFT and GPS common-view data.

Figure 9 shows $\mathrm{Log}_{10}\mathrm{TDEV}(\hat{e}_1)$ plotted against $\mathrm{Log}_{10}(\tau)$ for averaging times between 1 and 10^5 for the cases:

a) Three time transfer links of type C
b) Three time transfer links of type D
c) Six time transfer links, three of type C, and three of type D.

The long-term instabilities in the type D links (Figure 11) were significantly smaller than those for the type C links (Figure 10). There were, however, noticeable short-term instabilities due to the presence of clock noise at the epochs where time transfer measurements were not present. The use of all six links in the TTKF algorithm results in an appreciable improvement in both stability and error over medium and longer averaging times (Figure 12).

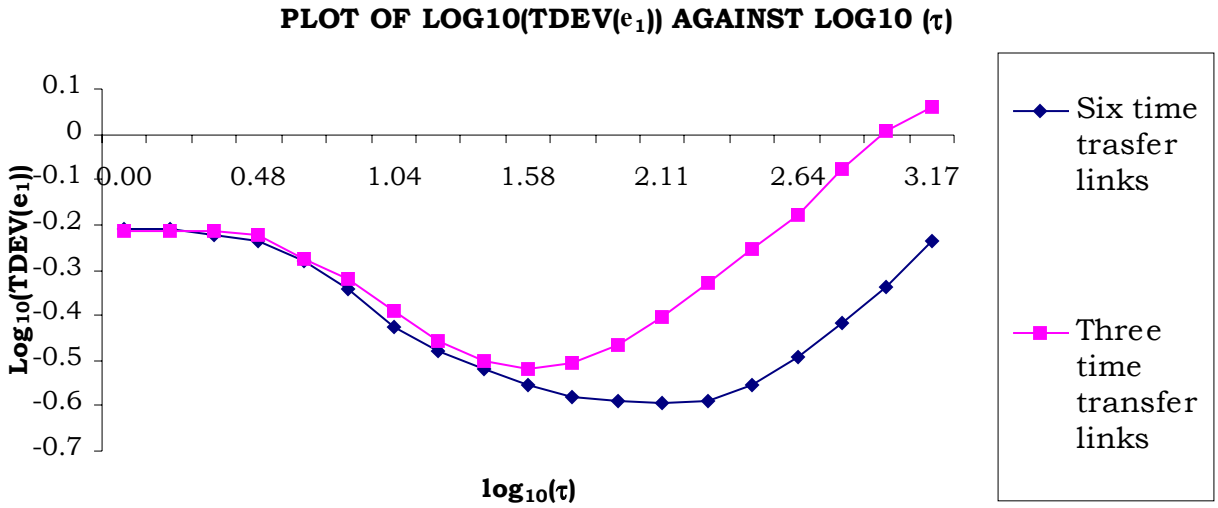

Figure 9. $\mathrm{Log}_{10}(\mathrm{TDEV}(\hat{e}_1))$ plotted against $\mathrm{Log}_{10}(\tau)$ for three time transfer links of type C and six time transfer links.

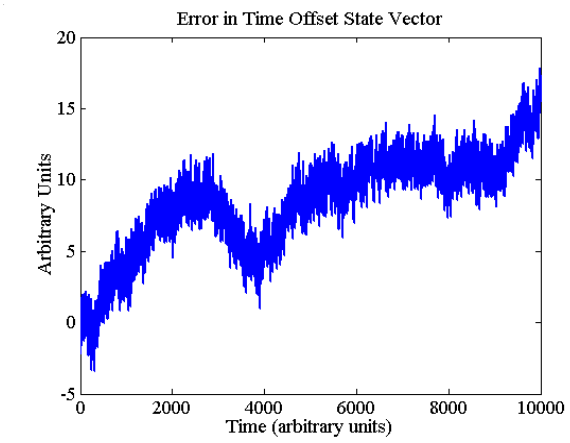

Figure 10. Example of the time-offset error when using three links of type C.

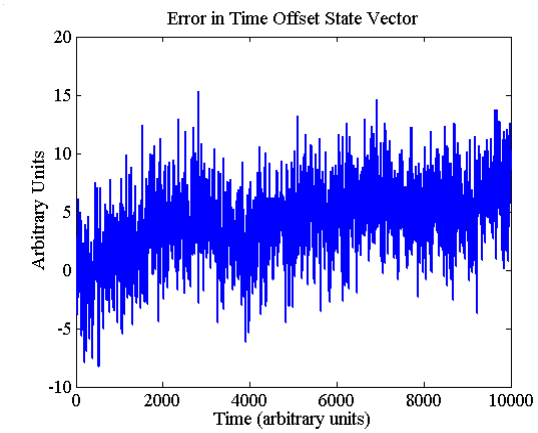

Figure 11. Example of the time-offset error when using three links of type D.

7. FUTURE DEVELOPMENT OF THE ALGORITHM

The work on this TTKF algorithm may be continued in several directions:

a) The study to date has assumed that only integer noise processes are present. The use of fractional noise processes, in particular the description of clock noise as Flicker Phase Modulation and the time-transfer link noise as Flicker Frequency Modulation, and the incorporation of these noise processes in the algorithm may be advantageous **[8]**.

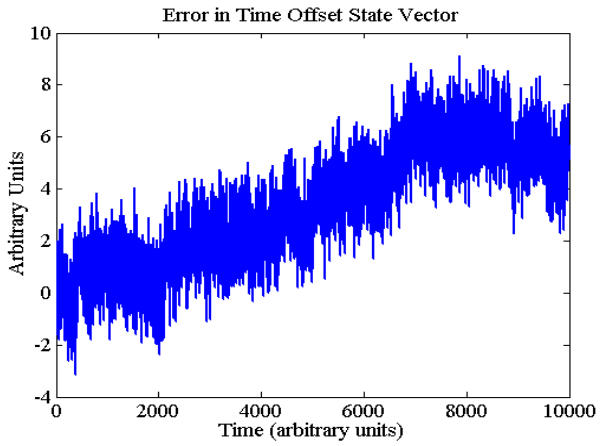

Figure 12. An example of the time-offset error obtained when using all six time transfer links.

b) Many measurement time series that will be used with this algorithm contain temperature-dependent instabilities. These instabilities do not correspond to a standard noise process. Work is required to determine how best to incorporate these effects into the TTKF algorithm.

c) The performance of a Kalman filter depends critically on the sufficiently accurate determination of the elements of the process covariance matrix Q and the measurement covariance matrix R. Methods to resolve and determine noise coefficients have been described **[9]**. That work needs to be extended and applied to the TTKF algorithm.

8. CONCLUSIONS

This work has studied the conditions of use of a Kalman filter to combine separate time-transfer link measurements made between two laboratories, with the aim of producing an optimal composite measurement. Time-transfer link biases are treated as additional state vector elements in this formulation. Using simulated data the resulting time-transfer Kalman filter algorithm has been shown to produce a composite time-transfer measurement that is more stable in both the short and long term than any of the component measurements. The simulations do, however, assume that the measurement and associated clock noise contains noise of integer noise types, where the noise parameters are known. The use of a pseudo-measurement is shown to improve further the stability of the algorithm. The addition and removal of time transfer links is shown to be relatively straightforward, as is the use of the filter with missing data and the inclusion of time transfer links with widely differing measurement intervals. Possible future improvements to the algorithm have been discussed. The ultimate test of the algorithm will be its performance on real time-transfer data. Such testing will be undertaken at NPL shortly.

REFERENCES

[1] D. Kirchner, 1991, *"Two-way time transfer via communication satellites,"* **Proceedings of the IEEE**, Special Issue on Time and Frequency, **79**, 983-990.

[2] R. Dach, T. Schildknecht, T. Springer, G. Dudle, and L. Prost, 2002, *"Continuous time transfer using GPS carrier phase,"* **IEEE Transactions on Ultrasonics, Ferroelectrics, and Frequency Control, 49**, 1480-1490.

[3] W. Lewandowski and C. Thomas, 1991, *"GPS time transfer,"* **Proceedings of the IEEE, 79,** 991-1000.

[4] W. Lewandowski, J. Azoubib, M. Weiss, V. Zhang, V.Hanns, A. G. Gevorkyan, P. P. Bogdanov, N. Tutolmin, J. Danaher, G. De Jong, J. Hahn, and M. Miranian, 1997, *"Glonass time transfer and its comparison with GPS,"* in Proceedings of the 11th European Frequency and Time Forum (EFTF), 4-6 March 1997, Neuchâtel, Switzerland, pp. 187-193.

[5] D. Kaplan, 1996, **Understanding GPS, Principles and Applications** (Artech House, Norwood, Massachusetts), pp. 391–409.

[6] K. R. Brown, 1991, *"The theory of the GPS composite clock,"* in Proceedings of the ION GPS-91 Meeting, 11-13 September 1991, Albuquerque, New Mexico, USA (Institute of Navigation, Alexandria, Virginia), pp. 223-241.

[7] S. T. Hutsell, 1996, *"Relating the Hadamard variance to MSC Kalman filter clock estimation,"* in Proceedings of the 14th Annual Precise Time and Time Interval (PTTI) Applications and Planning Meeting, 29 November-1 December 1995, San Diego, California, USA (NASA CP-3334), pp. 291-301.

[8] L. S. Schmidt, 2003, *"Atomic clock models using fractionally integrated noise structures,"* **Metrologia, 40** (3), in press.

[9] P. M. Harris, J. A. Davis, M. G. Cox, and S. L. Shemar, 2003, *"Least-squares analysis of two-way satellite time and frequency transfer measurements,"* **Metrologia, 40** (3), in press.

QUESTIONS AND ANSWERS

DEMETRIOS MATSAKIS (U.S. Naval Observatory): I was very curious about your constraint equation summing all the biases to zero. That correlates 100% with the time scale difference. I was wondering why it made a difference for that range of sampling times. I think I know the reason. It is because the data come in asynchronously, so you are not sampling all your biases at once. Is that right?

JOHN DAVIS: When I use the biases on the runs I do without, we have got all the epochs complete, so each epoch has separate measurements. What I think it actually comes from is from back here with this confusion. I think it is a little bit like the situation that you have got with a clock algorithm, when we are no longer directly measuring what we are trying to determine. With each measurement, we are measuring the time offset plus the bias of that particular link. What I was trying to do in the constraint was actually fill the filter, so in the long term the sum of the biases stay at a minimum.

YURIY SHMALLY (Guanajuato University): Could you please say what is actually a time-error model in your filter? And how many states do you filter?

DAVIS: In the states, I have three that represent the clock. And we have one for each time transfer link because of these biases that occur on them.